

## Variational Approach to Hard Sphere Segregation Under Gravity

Joseph A. Both and Daniel C. Hong

Physics, Lewis Laboratory, Lehigh University, Bethlehem, Pennsylvania 18015

### Abstract

It is demonstrated that the minimization of the free energy functional for hard spheres and hard disks yields the result that excited granular materials under gravity segregate not only in the widely known “Brazil nut” fashion, i.e. with the larger particles rising to the top, but also in reverse “Brazil nut” fashion. Specifically, the local density approximation is used to investigate the crossover between the two types of segregation occurring in the liquid state, and the results are found to agree qualitatively with previously published results of simulation and of a simple model based on condensation.

Segregation of hard sphere mixtures has a long history, starting perhaps from the classic papers by Wood and Jacobson [1], followed by Lebowitz, Rowlinson, and Widom [2,3], extending to the most recent works by various groups [4]. It is still controversial whether or not hard sphere mixtures do phase segregate in the absence of gravity [4]. However, in the presence of gravity, the situation is rather clear cut. Rosato et al. [5] advanced an explanation of the segregation in vertically shaken mixtures of granular materials by appealing to geometrical reorganization: during shaking, voids opening beneath larger particles are filled more readily by smaller particles. This may be contrasted with the apparent “buoyancy” of larger particles [6], or convection driven segregation [7]. But recent molecular dynamics simulations of weakly dissipative hard sphere and hard disk granular systems under gravity that are in global thermal equilibrium with a heat reservoir have shown that a reverse segregation phenomenon occurs as well [7]. These results were interpreted in light of a recent proposal that the hard spheres undergo condensation transition under gravity [8], which was subsequently tested by Molecular Dynamics simulations [10].

The density profile in the condensed regime is fairly uniform at the level of Enskog approximation [8], or displays oscillatory structure in the weighted density functional approximation [9, 11], which is consistent with the experimental observation of the formation of crystalline structure with fairly

uniform density near the bottom of the shaken granular materials [18]. It was argued that the type of segregation (Brazil nut [BN] or reverse Brazil nut [RBN]) results from a competition between the system's tendency to reorganize geometrically in the ways described by Rosato et al. [5] and the tendency of hard spheres under gravity to condense at low enough kinetic temperature [8-10]. It was suggested as a qualitative model [7] that in a binary hard sphere mixture, the particles belonging to the different species would be characterized by different condensation temperatures, so that during quenching from high to low temperature, the species with highest would tend to condense at the bottom of the sample first, leading ultimately to vertical segregation if this tendency were realized. This condensation driven tendency toward segregation, however, would be either augmented or opposed by the essentially geometric mechanisms identified by Rosato et al., which favor BN segregation only, depending respectively upon whether the smaller particle has higher or lower condensation temperature than the larger particle. The purpose of this Letter is to present for the first time a theory based on the variational principle and directly derive the phase boundary of the binary mixtures.

**Theory :** We calculate in the local density approximation (LDA). Specifically, with  $\psi_{id}$  being the Helmholtz free energy per particle for the ideal gas in the absence of gravity, and  $\psi_{exc}$  being that of the excess component due to particle interactions, the binary mixture free energy per area functional is given as a function of the densities  $\rho_i(\mathbf{r})$ :

$$\begin{aligned} \bar{F}[\rho_1(z), \rho_2(z)] = & \int_0^\infty dz \rho(z) \psi_{id}(\rho_1, \rho_2) + \\ & \int_0^\infty dz \rho(z) \psi_{exc}(\rho_1, \rho_2) + \\ & m_1 g \int_0^\infty dz \rho_1 z + m_2 g \int_0^\infty dz \rho_2 z, \end{aligned} \quad (1)$$

where 1 and 2 are particle indexes, and the total density,  $\rho$ , is the sum of the two:  $\rho = \rho_1 + \rho_2$ . This gives the free energy of a columnar sample of the system whose transverse cross section has one unit of area. The plane  $z = 0$  is the bottom of the container, and for the problem to be strictly one dimensional, the size of the container in the transverse direction must be infinite. Minimizing  $\bar{F}$  under the global constraints that the number of

particles of each species is conserved:

$$N_i = \int_V d\mathbf{r} \rho_i(\mathbf{r}), \quad i = 1, 2 \quad (2)$$

yields the desired density profiles.

The forms of  $\psi_{id}$  are given in [12] and it is standard [12, 13] that if  $Z \equiv \frac{P}{\rho T}$ , then

$$\frac{\psi_{exc}}{T} = \int_0^\rho (Z(\rho') - 1) \frac{d\rho'}{\rho'}. \quad (3)$$

For the form of  $Z$ , we use a generalized Carnahan-Starling equation of state, the so called Mansoori, Carnahan, Starling, Leland approximation for a finite number of hard sphere species [14]. Defining  $\xi_\alpha = \frac{\pi}{6} \sum_{i=1}^n \rho_i D_i^\alpha$  ( $\alpha = 0, \dots, 3$ ), with  $\rho_i = N_i/V$ , and  $n$  being the number of species in the mixture,  $Z$  is then given by

$$Z = \frac{6}{\pi \rho} \left[ \frac{\xi_0}{1 - \xi_3} + \frac{3\xi_1\xi_2}{(1 - \xi_3)^2} + \frac{3\xi_2^3}{(1 - \xi_3)^2} - \frac{\xi_3\xi_2^3}{(1 - \xi_3)^3} \right], \quad (4)$$

where  $\rho = \sum_{i=1}^n \rho_i$ . To perform the integration specified in Eq. (3) for  $n = 2$ , we recognize that this is an expression for the excess free energy for a homogeneous mixture in which  $\rho_1$  and  $\rho_2$  are *fixed* fractions of  $\rho$ , i.e.  $\rho_1/\rho$  and  $\rho_2/\rho$  are both constants. Then one readily sees then that the quantities  $\xi_i$  may be written as constant multiples of  $\rho$  only, viz.  $\xi_\alpha = C_\alpha \rho$ , which defines the constant  $C_\alpha$  in terms of  $\rho_1, \rho_2$  and  $D_1$  and  $D_2$ .

Performing the integration specified in Eq. (3) with the substitution of these relations, we find the desired form for  $\psi_{exc}$ :

$$\frac{\psi_{exc}}{T} = \left( \frac{\xi_2^3}{\xi_0 \xi_3^2} - 1 \right) \ln(1 - \xi_3) + \frac{3\xi_1\xi_2}{\xi_0(1 - \xi_3)} + \frac{\xi_2^3}{\xi_0 \xi_3(1 - \xi_3)^2}, \quad (5)$$

(see refs. [15] and [16]). This done, the functional  $\bar{F}[\rho_1(z), \rho_2(z)]$  defined in Eq. (1) is then fully specified. Its minimization is accomplished by solving for  $\rho_1(z)$  and  $\rho_2(z)$  the two equations ( $i = 1, 2$ ):

$$\frac{\delta \bar{F}}{\delta \rho_i} = \frac{d[\rho \psi_{id}]}{d\rho_i} + \psi_{exc} + \rho \frac{d\psi_{exc}}{d\rho_i} + m_i g z = \lambda_i, \quad (6)$$

where the Lagrange multipliers  $\lambda_i$  are introduced to constrain the minimization according to Eq. (2). These equations, though only algebraic, are nonlinear and highly nontrivial and must therefore be solved numerically via an

iterative scheme for  $\rho_i(z)$  at several points  $z$ . The two dimensional problem is solved analogously. We use the equation of state of hard disks used by Jenkins and Mancini [17]

$$Z = 1 + \frac{K_{11}}{\sigma_1^2} + 8 \frac{K_{11}}{\sigma_{12}^2} + \frac{K_{22}}{\sigma_2^2}, \quad (7)$$

where  $\sigma_i = D_i/2$  and  $\sigma_{ij} = \sigma_i + \sigma_j$ , and where

$$K_{ij} = \frac{\pi}{8} \rho_i \rho_j \sigma_{ij}^4 g_{ij}. \quad (8)$$

The functions  $g_{ij}$  are the pair correlations at contact. Following Jenkins and Mancini [17], we use

$$\begin{aligned} g_{11} &= \frac{1}{1-\eta} + \frac{9}{16} \frac{\eta_1 + \eta_2 R}{(1-\eta)^2} \\ g_{22} &= \frac{1}{1-\eta} + \frac{9}{16} \frac{\eta_1 + \eta_2 R}{R(1-\eta)^2} \\ g_{12} &= \frac{1}{1-\eta} + \frac{9}{8} \frac{\eta_1 + \eta_2 R}{(1+R)(1-\eta)^2} \end{aligned} \quad (9)$$

where  $\eta_i = \frac{\pi}{4} D_i^2 \rho_i$ , the area fraction of species  $i$ ,  $\eta = \eta_1 + \eta_2$ , and  $R = D_1/D_2$ . Eq. (3) is integrated, again using the fact that the fractions  $\rho_i/\rho$  are constant and then equations analogous to Eq. (6) are then solved iteratively for  $\rho_i(z)$ , where the derivatives of  $\psi_{exc}$  are evaluated numerically.

**Results and Discussion:** The control parameters that directly enter this formulation of the problem are  $g$ ,  $T$ ,  $m_i$ ,  $D_i$ , and  $\lambda_i$ . In practice, for any choice of  $g$ ,  $T$ ,  $m_i$ ,  $D_i$ , and  $\mu_i$ , the last of which control the average particle density, the parameters  $\lambda_i$  are tuned so that the integrated density profiles yield desired layer numbers  $\mu_i$  according to  $\mu_i = D_i^{d-1} \int dz \rho_i$ , where  $d$  is the dimensionality of the system. To show that the LDA is capable of generating reliable results, we present Fig. 1, which shows volume fraction profiles  $\eta_i(z) = \frac{\pi}{6} D_i^3 \rho_i(z)$  for  $d = 3$ ,  $D_1 = D_2 = 0.001$  m,  $m_1 = 1.047 \times 10^{-6}$  kg,  $m_2 = 2m_1$ ,  $g = 9.8$  m/s<sup>2</sup> generated by the LDA (lines) and generated by MD simulation (symbols) used in ref. [7]. The layer numbers  $\mu_1$  and  $\mu_2$  are both nominally 8, but the integrals of the LDA curves disagree slightly with those of the MD curves as a result of a systematic binning error in the MD results. The temperatures of the two systems differ;  $T_{LDA}/m_2 g D_2 \mu_2 = 0.0731$  and  $T_{MD}/m_2 g D_2 \mu_2 = 0.1401$ . The LDA system is not at all dissipative, so it is

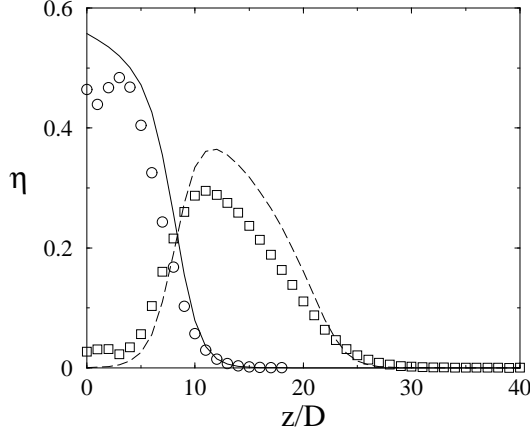


Figure 1: A comparison of density profiles calculated from the LDA (lines) and from molecular dynamics simulation (symbols). The dashed line and squares designate species 1, and the solid line and circles designate species 2;  $m_2/m_1 = 2$ ;  $D_2/D_1 = 1$ ;  $\mu_1 \approx \mu_2 \approx 8$ .

reasonable that the different systems give similar profiles only at *different* temperatures,  $T_{MD}$  being necessarily the higher one. We are, however, not able to exactly pin point the factor two difference in temperatures. The temperature difference notwithstanding, the resulting profiles are very similar, and indeed exhibit non-BN segregation. Note that in this case, the segregation mechanism cannot be geometric, because the particles are of equal size but with different mass.

In all subsequent work reported here, we choose  $g = 10 \text{ m/s}^2$ ,  $D_1 = 0.001 \text{ m}$ ,  $m_1 = 10^{-6} \text{ kg}$ , and  $\mu_i = 10$  to within less than one tenth percent. To investigate the dependence of segregation on mass and diameter ratios, we vary  $D_2$  and  $m_2$  such that  $D_2 \geq D_1$  and  $m_2 \geq m_1$ , find  $\eta_i(z)$  at low temperature, and quantify the segregation as a function of  $D_2/D_1$ ,  $m_2/m_1$ , and  $T$ . Our choice to quantify the segregation is simply the ratio of the centers of mass of the two species:  $\langle z_1 \rangle / \langle z_2 \rangle$ . Specifically,  $\langle z_1 \rangle / \langle z_2 \rangle < 1$  indicates BN segregation,  $\langle z_1 \rangle / \langle z_2 \rangle = 1$  indicates crossover, and  $\langle z_1 \rangle / \langle z_2 \rangle > 1$  indicates RBN segregation. To reduce the number of control parameters and to try to make some comparison with the condensation theory [7] which originally motivated this work, we choose to explore the lower temperature regimes at a fixed *reduced* temperature. Because the LDA cannot generate

information about the solid phase, we are careful to choose temperatures at which total volume fractions,  $\eta(z) = \eta_1(z) + \eta_2(z)$  have their maximum somewhere on the range 0.50 to 0.65 when  $d = 3$ , that is, near the density of the simple cubic packed single species solid ( $\eta \approx 0.52$ ), but not as dense as the hexagonally packed single species solid ( $\eta \approx 0.74$ ). When  $d = 2$ , the maximum of  $\eta(z)$  is kept on the range 0.80 to 0.85 (also between the square and triangular packing single species area fractions, approximately 0.79 and 0.91). Thus, our method explores fluid systems of moderate to high densities near the bottom of the sample. We have found that choosing a reduced temperature  $\tilde{T} \equiv T/(m_2 g D_2 \mu_2) = 0.0375$  ( $d = 3$ ) and  $\tilde{T} \equiv T/(m_2 g D_2 \mu_2) = 0.0300$  ( $d = 2$ ) keeps the maximum of  $\eta(z)$  on the prescribed ranges over the spectrum of diameter and mass ratios we have used.

Fig. 2 summarizes the results of our calculations for diameter ratios  $D_2/D_1 = 1.2, 1.5, 2.0, 3.0, 4.0$ , and a range of mass ratios for both  $d = 2$  and 3. If from these data we interpolate to find those values of  $m_2/m_1$  at which crossover occurs ( $\langle z_1 \rangle / \langle z_2 \rangle = 1$ ) for given values of  $D_2/D_1$ , we generate the data shown in Fig. 3. Each graph displays three curves. The dashed curves with symbols are the crossover curves calculated with the LDA at the low temperatures cited above and also at  $\tilde{T} = 0.1500$  for both  $d = 2$  and  $d = 3$ , so that the temperature dependence may be illustrated. To the left of a crossover curve, the segregation is of the BN variety; to the right, it is RBN. Thus, the LDA reveals that as reduced temperature increases, an increasingly larger region of parameter space gives rise to RBN segregation. Indeed, if we assume that in the high temperature limit the density of each species is proportional to  $\exp(-m_i g z / T)$ , then for  $\mu_1 = \mu_2$ , one may calculate for  $d = 2$  and  $d = 3$  that the ratio of centers of mass is given by

$$\frac{\langle z_1 \rangle}{\langle z_2 \rangle} = \frac{m_2}{m_1}, \quad (10)$$

which indicates the crossover curve is the vertical line  $\frac{m_2}{m_1} = 1$ , a result consistent with the trend in the LDA results presented in Fig. 3.

Also appearing on the both graphs in Fig. 3 as solid lines are crossover curves predicted from the simple condensation argument. Briefly, these are obtained by assuming the ratio of condensation temperatures in the single species theory

$$T_{c2}/T_{c1} = m_2 g D_2 \mu_2 / m_1 g D_1 \mu_1$$

measures the tendency of species 2 to segregate to the bottom at  $T < T_{c2}$  due to the condensation mechanism [7].

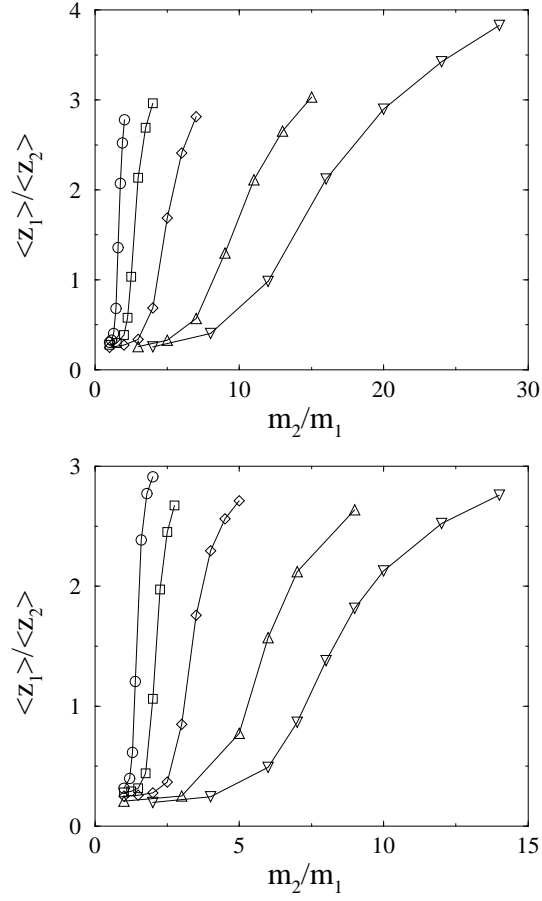


Figure 2: Segregation parameter  $\langle z_1 \rangle / \langle z_2 \rangle$  as a function of mass ratio  $m_2/m_1$  for hard spheres (left) and hard disks (right). In both graphs  $\mu_1 = \mu_2 = 10$ ;  $D_2/D_1 = 1.2$  (circle), 1.5 (square), 2.0 (diamond), 3.0 (up triangle), 4.0 (down triangle).  $\tilde{T}_{3d} = 0.0375$ ;  $\tilde{T}_{2d} = 0.0300$ .

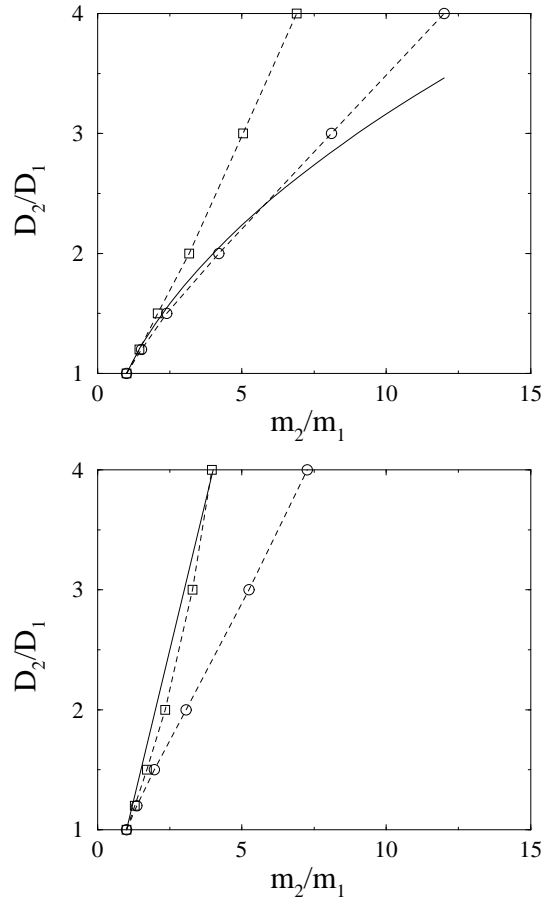


Figure 3: Curves through parameter space along which the segregation parameter  $\langle z_1 \rangle / \langle z_2 \rangle = 1$ , indicating the crossover from BN (left) to RBN (right) segregation, for  $d = 3$  (upper) and for  $d = 2$ . The dashed curves marked by circles are from linear interpolation of the data shown in Fig. 2, and are for the low temperatures given in the text. The dashed curves marked by squares are for higher reduced temperature ( $\tilde{T} = 0.1500$  in both cases).



If we choose to equate this with Rosato et al.'s [5] control parameter for the reorganization,  $(D_2/D_1)^d$ , we can obtain the crossover curve (The solid lines in Fig. 3). We see fair agreement with our theoretical prediction at low reduced temperature for  $d = 3$ , but significant disagreement appears at  $m_2/m_1 \approx 7$ ; the crossover curve seems practically linear, in disagreement with the scaling suggested by the condensation argument. For  $d = 2$ , the low temperature LDA boundary is linear, in agreement with the scaling suggested by the condensation argument, but that argument of course cannot predict the slope. Moreover, the LDA computed boundaries are necessarily temperature dependent, but the condensation theory [7] does not predict a temperature dependence. Thus, although the condensation theory has been useful in directing us to look for certain dependencies and, indeed, for the phenomenon of RBN segregation itself, its utility, except as a heuristic, is somewhat circumscribed. However, the equilibrium approach of minimizing Helmholtz free energy seems a promising theoretical alternative, as it is capable of generating solutions in good agreement with those obtained from MD simulation, as in Fig. 1.

## References

- [1] W.W. Wood and J. D. Jacobson, J. Chem. Phys. **27**, 1207 (1957).
- [2] J. Lebowitz and J.S Rowlinson, J. Chem. Phys. **41**, 133 (1964).
- [3] B. Widom and J. S. Rowlinson, J. Chem. Phys. **52**, 1670 (1970).
- [4] M. Dijkstra, R. von Roji, and R. Evans. Phys. Rev. E. **51**, 5744 (1999).
- [5] A. Rosato, et al., Phys. Rev. Lett. **58**, 1038 (1987).
- [6] T. Shinbrot and F. Muzzio, Phys. Rev. Lett. **81**, 4365 (1998).
- [7] D. C. Hong, P. V. Quinn and S. Luding, Phys. Rev. Lett. **86**, 3423 (2001).
- [8] D. C. Hong, Physica A **271**, 192 (1999).
- [9] J. A. Both and D. C. Hong, Phys. Rev. E **64**, 061105 (2001).
- [10] P. V. Quinn and D. C. Hong, Phys. Rev. E **62**, 8295 (2000).
- [11] P. Tarazona, Mol. Phys **52**, 81 (1984).
- [12] P. M. Morse, *Thermal Physics*, Addison-Wesley Publishing Co., Redwood City, CA, 1969.
- [13] J. P. Hansen and I. R. McDonald, *Theory of Simple Liquids*, Academic Press, New York, 1976.
- [14] G. A. Mansoori, et al., J. Chem. Phys. **54**, 1523 (1971).
- [15] J. J. Salacuse, G. Stell, J. Chem. Phys **77**, 3714 (1982).

- [16] A. Meroni, A. Pimpinelli, L. Reatto, J. Chem. Phys **87**, 3644 (1987).
- [17] J. T. Jenkins and F. Mancini, J. Appl. Mech. **54**, 29, (1987).
- [18] T. Biben, R. Ohnesorge and H. Lowen, Europhys. Lett. **71**, 615 (1993).